International Journal of Cardiology xxx (2017) xxx–xxx

Contents lists available at ScienceDirect

International Journal of Cardiology

journal homepage: www.elsevier.com/locate/ijcard

The effect of bioresorbable vascular scaffold implantation on distal coronary endothelial function in dyslipidemic swine with and without diabetes☆

Mieke van den Heuvel [a,b,d,1], Oana Sorop [a,d,1], Nienke S. van Ditzhuijzen [a,1], René de Vries [b,1], Richard W.B. van Duin [a,1], Ilona Krabbendam-Peters [a,1], Janine E. van Loon [a,c,1], Moniek P. de Maat [c,1], Heleen M. van Beusekom [a,1], Wim J. van der Giessen [a,d,2], A.H. Jan Danser [b,1], Dirk J. Duncker [a,d,*,1]

[a] Department of Cardiology, Thoraxcenter, Erasmus University Medical Center, Rotterdam, The Netherlands
[b] Department of Internal Medicine, Sector Pharmacology and Metabolic Diseases, Erasmus University Medical Center, Rotterdam, The Netherlands
[c] Department of Hematology, Erasmus University Medical Center, Rotterdam, The Netherlands
[d] Netherlands Heart Institute, Utrecht, The Netherlands

ARTICLE INFO

Article history:
Received 20 June 2017
Received in revised form 3 October 2017
Accepted 13 November 2017
Available online xxxx

Keywords:
Bioresorbable vascular scaffold
Endothelial function
Diabetes

ABSTRACT

Background: We studied the effect of bioresorbable vascular scaffold (BVS) implantation on distal coronary endothelial function, in swine on a high fat diet without (HFD) or with diabetes (DM + HFD).
Methods: Five DM + HFD and five HFD swine underwent BVS implantation on top of coronary plaques, and were studied six months later. Conduit artery segments >5 mm proximal and distal to the scaffold and corresponding control segments of non-scaffolded coronary arteries, as well as segments of small arteries within the flow-territories of scaffolded and non-scaffolded arteries were harvested for in vitro vasoreactivity studies.
Results: Conduit segments proximal and distal to the BVS edges showed reduced endothelium-dependent vasodilation as compared to control vessels ($p < 0.01$), with distal segments being most prominently affected ($p < 0.01$). Endothelial dysfunction was only observed in DM + HFD swine and was principally due to a loss of NO. Endothelium-independent vasodilation and vasoconstriction were unaffected. Surprisingly, segments from the microcirculation distal to the BVS showed enhanced endothelium-dependent vasodilation ($p < 0.01$), whereas endothelium-independent vasodilation and vasoconstriction were unaltered. This enhanced vasorelaxation was only observed in DM + HFD swine, and did not appear to be either NO- or EDHF-mediated.
Conclusions: Six months of BVS implantation in DM + HFD swine causes NO-mediated endothelial dysfunction in nearby coronary segments, which is accompanied by a, possibly compensatory, increase in endothelial function of the distal microcirculation. Endothelial dysfunction extending into coronary conduit segments beyond the implantation-site, is in agreement with recent reports expressing concern for late scaffold thrombosis and of early BVS failure in diabetic patients.

Drug-eluting stents (DES) are widely used for the treatment of obstructive coronary artery disease (CAD), including in patients with diabetes mellitus (DM) [1]. However, the use of, in particular first generation, DES has raised concern regarding long-term endothelial dysfunction adjacent to the stent including the distal microcirculation [2,3], which could be related to adverse events including late stent thrombosis [4]. Second generation DES have partially succeeded in reducing thrombosis, however paradoxical vasoconstriction adjacent to the stent has still been reported [4–6].

The everolimus-eluting bioresorbable vascular scaffold (BVS) has been introduced with the aim to provide temporary vessel scaffolding and to be subsequently resorbed over time with restoration of vasomotion. Indeed, the ABSORB trials have demonstrated efficacy for the treatment of simple CAD in selected DM and non-DM patients up to five years with some restoration of vasomotion [7–10]. Conversely, paradoxical vasoconstriction has also been observed within the scaffold and adjacent segments even at five years after implantation [7,8],

☆ This study was partly supported by a grant from Abbott Vascular (Grant No: CP001 / EMC 109-09-03).
* Corresponding author at: Division of Experimental Cardiology, Department of Cardiology, Thoraxcenter, Erasmus University Medical Center, PO Box 2040, 3000 CA Rotterdam, The Netherlands.
E-mail address: d.duncker@erasmusmc.nl (D.J. Duncker).
[1] These authors take responsibility for all aspects of the reliability and freedom from bias of the data presented and their discussed interpretation.
[2] Deceased 6 June 2011.

https://doi.org/10.1016/j.ijcard.2017.11.037

indicating persisting impairment of endothelial function. Of concern, higher rates of BVS thrombosis have recently been reported in unselected populations and in meta-analyses of all randomized trials up to 24 months after BVS implantation as compared to a specific second generation DES [11–13], as well as lack of superior vasomotor reactivity after 36 months [14] and still incomplete vasomotion after 5 years [9]. Therefore, endothelial dysfunction with its subsequent associated adverse events still remains an issue, also after BVS implantation. Moreover, whether BVS affects endothelial function in the distal perfusion territory of the scaffold is presently unknown. This is of importance since a healthy microcirculation plays a key role in the regulation of optimal myocardial perfusion [15], also after percutaneous coronary intervention (PCI).

A significant proportion of PCIs involves DM patients that experience a higher incidence of treatment failure, including stent thrombosis [1]. Indeed, DM has been shown to be an independent predictor of revascularisation failure six months after BVS implantation [11]. DM and endothelial dysfunction are closely related [16]. However, in the setting of DM, detailed studies of endothelial function of both coronary macro- and micro-circulation in the restoration phase of the BVS are currently lacking.

Swine are an excellent model for the evaluation of coronary scaffolds because of the anatomical similarities between porcine and human coronary arteries [17,18]. In addition, DM-induction in combination with a high fat diet (HFD) is known to generate atherosclerosis, and specific components of endothelial function can be studied to unravel underlying mechanisms [19,20]. Although the effects of BVS implantation have been studied in healthy swine, showing resemblance to the human situation including lack of vasomotion of the scaffold six months after implantation [17,18], details regarding endothelial function in the restoration phase in an atherosclerosis model with and without DM are currently lacking. Consequently, the present study was undertaken to evaluate in vitro the effect of BVS on adjacent endothelial function, as well as of the distal microcirculation, six months after implantation in dyslipidemic swine with or without DM.

1. Methods

1.1. Study device

The ABSORB™ BVS (Abbott Vascular, USA) is a balloon-expandable, fully bioresorbable scaffold that consists of a poly (L-lactide) backbone with a poly (D,L-lactide) coating in a 1:1 ratio with everolimus.

1.2. Experimental design

The protocol was approved by the local animal ethics committee and the study was performed according to the National Institutes of Health guide for the care and use of Laboratory animals. The protocol has been described in detail elsewhere [19–21]. In short, ten male crossbred (Yorkshire × Landrace) swine were fed a cholesterol-rich diet (HFD). Five animals were rendered DM (DM + HFD) by a single-dose injection of streptozotocin. After nine months of atherogenesis, quantitative coronary angiography (QCA) was performed. All anesthetized swine (isoflurane, 1–2.5% *v/v*) received randomly assigned single 3.0 × 18.0 mm BVS implants in two epicardial coronary arteries with a scaffold to artery ratio of 1.1 on top of an atherosclerotic lesion, based on the angiogram, with follow up (FU) of six months. The untreated coronary artery served as a control. After stent implantation, all swine received acetylsalicylic acid (300 mg) and clopidogrel (75 mg) once daily. Blood samples were obtained, as published previously [19,20]. Also, plasma von Willebrand factor (vWf) levels were determined as described previously [22].

At six months FU, QCA was repeated in anesthetized swine (pentobarbital sodium 20 $mg \cdot kg^{-1} \cdot h^{-1}$) and afterwards they were euthanized. The hearts were excised and placed in Krebs buffer [3,19]. Of each animal, one coronary artery treated with a BVS and one untreated artery were used. Segments of epicardial conduit arteries (>2 mm diameter) of a BVS treated artery, located >5 mm proximal or distal to the scaffold's edges, were isolated. Also, segments of the untreated artery at approximately similar locations were obtained. In addition, segments of epicardial small arteries (~300 μm diameter) in the distal flow area of the scaffold and of a similar location of the untreated control artery were dissected out for subsequent functional studies. The scaffold, including immediately adjacent ~5 mm proximal and distal vessel segments, was used in a separate study [21].

1.3. Quantitative coronary angiography

QCA analysis was performed by the Coronary Angiographic Analysis System (CAAS, version 5.9.2 Pie Medical Imaging BV, The Netherlands). After maximal vasodilation with isosorbide dinitrate (1 mg/artery i.c.), minimal and maximal lumen diameter were measured both proximal and distal to the BVS and in corresponding segments of unscaffolded reference coronary arteries.

1.4. In vitro coronary conduit and small arterial function assessment

Segments of conduit arteries (~4 mm length) were suspended in organ baths. Segments of small arteries (~2 mm length) were mounted in Mulvany wire-myographs (DMT, Denmark). Vascular responses were measured as changes in isometric force. Both conduit and small arteries were subjected to the same experimental protocol as described previously [3,19]. In short, after determination of the maximal contractile response to 0.1 mol/l potassium chloride (KCl), concentration-response curves (CRCs) were acquired using separate, in vivo adjacently positioned, segments. Endothelium-dependent relaxation to bradykinin (BK, 10^{-10}–10^{-6} mol/l) was recorded upon pre-constriction by the thromboxane analogue U46619 (10^{-6} mol/l) in a first set of segments. In order to determine nitric oxide (NO) dependent and NO-independent contributions, in a second set, the CRC for BK was constructed after 30 min of pre-incubation with the NO-synthase inhibitor *N*-nitro-L-arginine methyl ester (L-NAME, 10^{-4} mol/l) to block endogenous NO-production. From a third set, endothelium-independent but NO-mediated vasodilation to *S*-nitroso-*N*-acetylpenicillamine (SNAP, 10^{-9}–10^{-5} mol/l) was measured. Finally, CRCs for endothelin-1 (ET-1, 10^{-10}–10^{-7} mol/l) were constructed to study vasoconstriction in a fourth set of vessel segments.

In addition, small arteries were subjected to an extended protocol, due to availability of more vessel-segments and experimental set-ups, to study endothelial function in more detail. Additional sets of segments were incubated with the small conductance Ca^{2+}-activated K^+-channel inhibitor apamin (APA,10^{-7} mol/l), together with the intermediate conductance Ca^{2+}-activated K^+-channel inhibitor TRAM34 (10^{-5} mol/l) to block the endothelium-derived hyperpolarizing factor (EDHF) component of BK-induced relaxation [23] alone or in combination with L-NAME. This combination of blockers has previously been shown to almost completely abolish BK-induced vasodilation [19]. All reagents used were obtained from Sigma-Aldrich, The Netherlands.

1.5. Histology

Finally, conduit arterial segments were formaldehyde-fixed and stained en face with Oil-red-O (Sigma, The Netherlands) as a macroscopic stain of fat accumulation or stained with resorcin-fuchsin as a microscopic overview stain. Morphometry of the Oil-red-O staining was performed by measuring total area and stained area with an image analysis system (Clemex Technologies Inc., Canada) and data are presented as percentage lipid area.

1.6. Data analysis

Values are presented as mean ± SEM. Differences between outcome variables were analysed using paired *t*-testing, after normal distribution of data was confirmed with Komolgorov-Smirnov normality test. Vasodilator responses to BK and SNAP were expressed as percentage of pre-constriction to U46619. Vasoconstriction to ET-1 was normalized to the response to 0.1 mol/l KCl. Statistical analysis of CRCs was performed using two-way ANOVA, followed by Bonferroni's post hoc correction (StatView). $P < 0.05$ (two-tailed) was considered statistically significant.

2. Results

2.1. Model characteristics

Both DM + HFD and HFD swine showed elevated cholesterol levels, and only DM + HFD swine showed high glucose levels [19–21]. Plasma vWf-levels increased over time in both DM + HFD (0.28 ± 0.02 IU/ml at implantation; 0.34 ± 0.01 IU/ml at 6 months FU, $p < 0.05$) and HFD swine (0.30 ± 0.04 IU/ml at implantation, 0.37 ± 0.02 IU/ml at 6 months FU, $p < 0.05$), without a difference between the groups ($p > 0.1$).

2.2. QCA analysis

At 6 months FU, calculated mean lumen diameters both proximal and distal to the BVS were similar between BVS-treated coronaries and corresponding segments in non-scaffolded coronaries in DM + HFD and HFD animals (example shown in Fig. 1A). Mean lumen diameters of vessels used in the functional experiments were similar between groups (DM + HFD proximal to BVS: 4.06 ± 0.25 vs. Control proximal: 3.38 ± 0.46 mm; DM + HFD distal to BVS: 2.66 ± 0.26 vs. Control distal: 2.37 ± 0.34 mm; HFD proximal to BVS: 3.53 ± 0.42 vs. Control proximal 3.50 ± 0.04 mm; HFD distal to BVS: 2.09 ± 0.18 vs. Control distal 2.74 ± 0.41 mm; all, $p > 0.1$).

Please cite this article as: M. van den Heuvel, et al., The effect of bioresorbable vascular scaffold implantation on distal coronary endothelial function in dyslipidemic swine with and ..., Int J Cardiol (2017), https://doi.org/10.1016/j.ijcard.2017.11.037

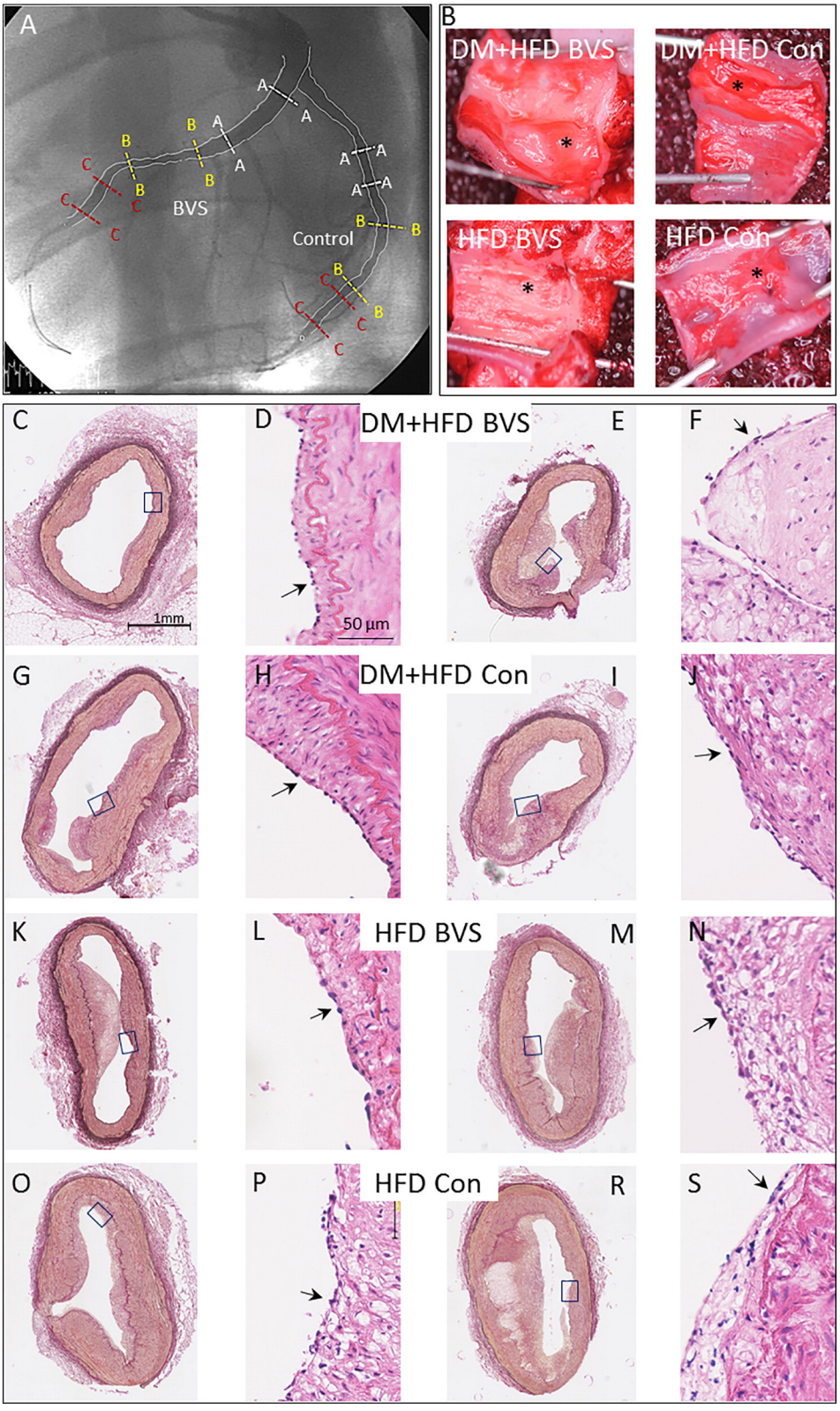

Fig. 1. Representative angiogram with depicted vessel segments located >5 mm proximal (delineated by the dashed white lines A–A) and distal (delineated by the dashed red lines C–C) to the BVS edges (delineated by the dashed yellow lines B–B), or corresponding segments of the reference (control) artery from which the mean lumen diameters were calculated (panel A). Representative segments (opened longitudinally), showing macroscopic fatty streaks, as visualized by en face Oil-red-O staining (panel B), and representative cross-sections (resorcin-fuchsin staining) showing plaques with different degrees of complexity from DM + HFD (panels C–J) and HFD (panels K–S) swine. *Indicates plaque. Arrows indicate endothelial lining. (For interpretation of the references to colour in this figure legend, the reader is referred to the web version of this article.)

Please cite this article as: M. van den Heuvel, et al., The effect of bioresorbable vascular scaffold implantation on distal coronary endothelial function in dyslipidemic swine with and ..., Int J Cardiol (2017), https://doi.org/10.1016/j.ijcard.2017.11.037

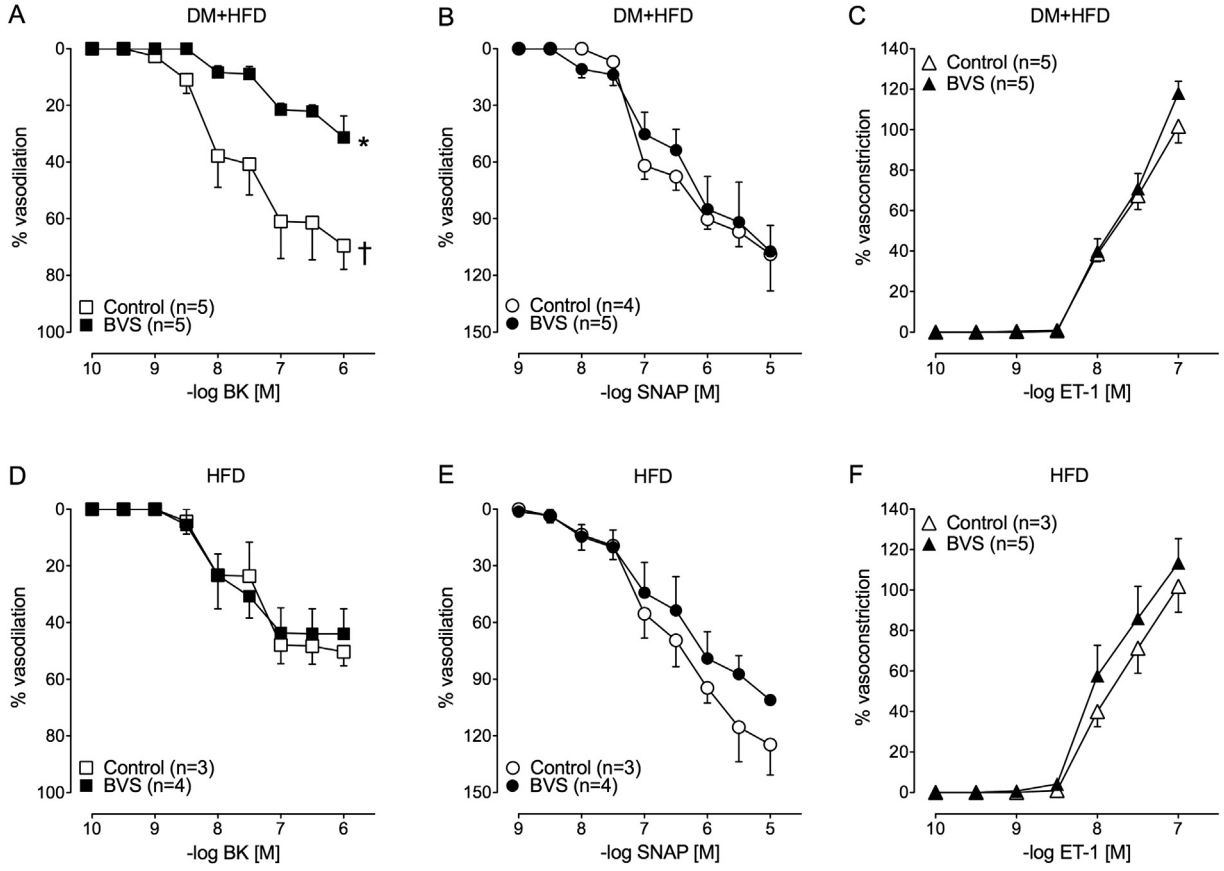

Fig. 2. Detailed coronary conduit artery function located >5 mm distal to the BVS and in control arteries, in dyslipidemic swine with or without DM. Figure highlighting the effects of six months of BVS implantation on BK-mediated vasodilation (A, D), SNAP-mediated vasodilation (B, E), and ET-1 mediated vasoconstriction (C, F) of distal conduit segments of DM + HFD (A-C) and HFD swine (D-F). Figure also highlighting the effect of DM + HFD on conduit arterial function of control segments (A–C) vs. HFD control segments (D–F). $^{*}p < 0.01$ DM + HFD BVS vs. DM + HFD Control; $^{\dagger}p = 0.051$ DM + HFD Control vs. HFD Control. BK = bradykinin, BVS = bioresorbable vascular scaffold, DM = diabetes mellitus, ET-1 = endothelin-1, HFD = high fat diet, n = number of animals, SNAP = *S*-nitroso-*N*-acetylpenicillamine.

2.3. In vitro vascular function

Contractile responses to KCl and U46619 were not significantly different between vessel segments of BVS-treated and control coronaries of DM + HFD and HFD swine, both for conduit and small arteries (data not shown).

2.3.1. Conduit arteries

DM on top of HFD slightly enhanced BK-induced dilation in control arteries (Fig. 2). BVS markedly blunted BK-induced vasodilation in DM + HFD swine, without altering the BK-response in HFD swine (Fig. 2). In accordance with previous studies from our laboratory [3], the BVS-induced attenuation of BK-mediated vasodilation was more pronounced in distal conduit artery segments as compared to proximal segments (Suppl. Fig. 1). Consequently, Fig. 2 only shows the responses in conduit artery segments located distal to the BVS, and vascular function was studied in more detail in these segments. Responses to SNAP and ET-1 were unaffected by either DM or BVS as compared to control vessels, indicating a BK-specific effect (Fig. 2).

L-NAME reduced BK-induced vasodilation under all conditions (Fig. 3). However, BVS significantly attenuated the surface area encompassed by the BK-response curves in the presence and absence of L-NAME in DM + HFD swine, so that the smallest NO-dependent area under the curve was observed in BVS treated vessels (25 ± 9), as compared to control vessels (101 ± 18) in DM + HFD swine and compared to BVS-treated vessels in HFD swine (56 ± 8; both $p < 0.05$). These observations indicate that loss of NO contributed to the blunted BK-induced vasodilation in conduit artery segments located >5 mm distal to the BVS in DM + HFD swine (Fig. 3).

2.3.2. Small arteries

In HFD swine, BVS did not alter the response to BK in small arteries of the microcirculation distal to the BVS (Fig. 4). However, in HFD + DM swine, BVS significantly enhanced the response to BK, both versus its own control and versus the BVS group of HFD swine (Fig. 4A, E). This difference remained apparent during L-NAME, TRAM34 and apamin, and the combination of these inhibitors. Inhibition of eNOS, with or without concomitant EDHF blockade, reduced the responses to BK, the largest reductions being observed in the presence of all inhibitors. However, this reduction appeared smaller in the BVS group of DM + HFD swine, indicating a remaining non-NO/non-EDHF mediated component of the BK-response, although this failed to reach statistical significance (Fig. 4A–H). Responses to SNAP (Fig. 4I, J) and ET-1 (Fig. 4K, L) were unaltered by either DM or BVS.

2.4. Histology

The Oil-red-O area was similar in conduit arterial segments located >5 mm distal to the BVS implant as compared to control coronary conduit arteries in both DM + HFD and HFD swine respectively

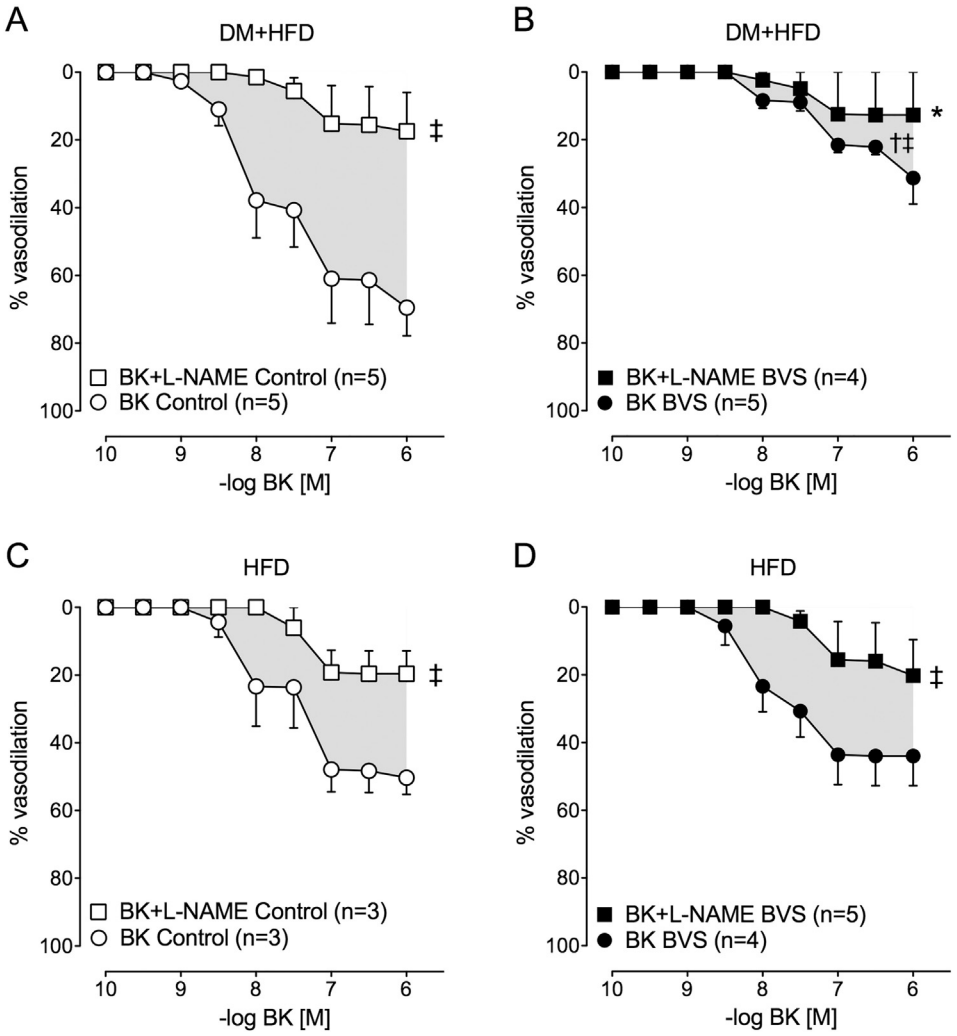

Fig. 3. NO- and non NO-mediated endothelial function located >5 mm distal to the BVS and in control arteries, in dyslipidemic swine with or without DM. Figure highlighting the effects of six months of BVS implantation on NO-mediated endothelium-dependent vasodilation of distal conduit segments of DM + HFD (A, B) and HFD swine (C, D). The grey area in between the BK and L-NAME curves depicts the specific contribution of the NO-mediated component of the BK-response. $^{*}p < 0.05$ area DM + HFD BVS vs. area DM + HFD Control; $^{\dagger}p < 0.05$ area DM + HFD BVS vs. area HFD BVS; $^{\ddagger}p < 0.05$ BK vs. BK + L-NAME. Abbreviations as in Fig. 2. In addition: L-NAME = *N*-nitro-L-arginine methyl ester, NO = nitric oxide.

(DM + HFD: BVS vs. Control: 30 ± 7% vs. 27 ± 8%, HFD: BVS vs. Control: 30 ± 6% vs. 26 ± 9%; all $p > 0.1$). Representative segments are shown in Fig. 1B.

As published previously [20], plaques with different degrees of complexity were observed to a similar extent in the coronary conduit arteries from DM + HFD and HFD swine, with presence of intact endothelium in both the lesion area as well as in the structurally unaltered vessel wall. Representative examples are shown in Fig. 1C–J, K–S. Also, as reported previously [19], coronary small arteries of both groups showed fatty streak lesions. The effect of BVS implantation on the atherosclerosis process distal to the BVS was not studied in detail in the present study.

3. Discussion

In the present study, we evaluated the effects of BVS implantation on endothelial function in vitro, of the vasculature located in the proximity (>5 mm from the edges) of the implanted BVS in a dyslipidemic swine model with or without DM. We hypothesized that the coronary circulation distal to the BVS would be at increased risk for endothelial dysfunction, especially in DM. The main findings were that: (i) only in the presence of DM, coronary conduit arteries showed decreased endothelium-dependent vasodilation, particularly distal to the BVS. This was principally due to loss of NO-mediated dilation; (ii) interestingly, the microcirculation within the distal perfusion territory showed slightly enhanced endothelium-dependent vasodilation that appeared to be independent of NO- or EDHF-mediated mechanisms.

In the present animal model, the high fat diet resulted in a similar degree of non-obstructive coronary atherosclerosis in DM + HFD compared to HFD swine [19,20], as well as increased plasma vWf-levels over time, indicating systemic endothelial dysfunction associated with CAD development [24]. In contrast, specific components of both systemic and coronary microvascular function were altered only in the presence of DM, similar to diabetic patients [19,25], making it a relevant model for the study of coronary interventions in the context of CAD and DM. BVS implantation within this model resulted in a similar vascular healing response with or without DM, with a heterogeneous coverage of the scaffold and a low polymer mass loss of the BVS at six months [21]. Therefore, the scaffold is likely to be immobile at this time-point according to prior results [8,18], although we did not perform vasomotion experiments to confirm this. For the present study, we focused on coronary vascular function in the segments located >5 mm from the scaffold's edges.

Please cite this article as: M. van den Heuvel, et al., The effect of bioresorbable vascular scaffold implantation on distal coronary endothelial function in dyslipidemic swine with and ..., Int J Cardiol (2017), https://doi.org/10.1016/j.ijcard.2017.11.037

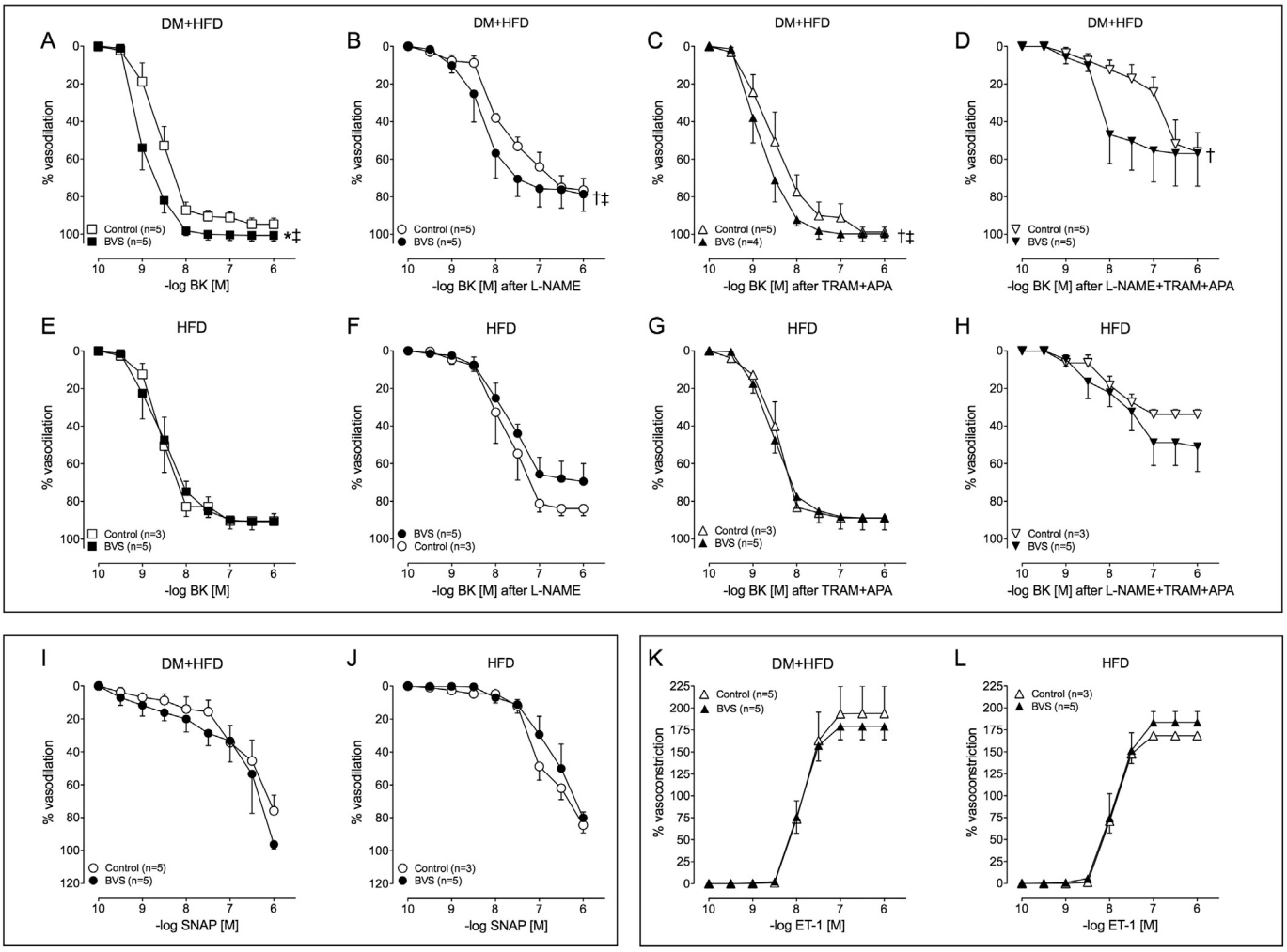

Fig. 4. Detailed coronary small arterial function in the distal perfusion area of the BVS and in control segments, in dyslipidemic swine with or without DM. Figure highlighting the effects of BVS on endothelium-dependent BK-induced vasodilation (A, E) after specific blockers (B, C, D, F, G, H), as well as endothelium-independent SNAP-induced vasodilation (I, J) and ET-1-induced vasoconstriction (K, L) of segments from the distal coronary microcirculation of DM + HFD (A, B, C, D, I, K) and HFD swine (E, F, G, H, J, L). Figure also highlighting the effect of DM + HFD on BK-mediated small arterial function distal to BVS (A) vs. BVS-treated vessels of HFD swine (E). L-NAME: blockage of endogenous NO (B, F). TRAM + APA: blockage of specific EDHFs (C, G). L-NAME + TRAM + APA: blockage of both endogenous NO and of specific EDHFs (D, H). $^{*}p < 0.01$ DM + HFD BVS vs. DM + HFD Control; $^{\dagger}p < 0.05$ DM + HFD BVS vs. DM + HFD Control; $^{\ddagger}p < 0.01$ DM + HFD BVS vs. HFD BVS. Abbreviations as in Fig. 2. In addition: EDHF = endothelium-derived hyperpolarizing factor, TRAM + APA = TRAM34 and apamin.

Only in swine with DM, we observed impaired coronary conduit endothelium-dependent vasodilation distal to the BVS. This impairment is in accordance with previous DES-studies, which also showed endothelial dysfunction in the peri-stent area, particularly in the distal segment, 6–16 months after implantation, in particular for first generation [2], and less extensively also for second generation [4–6] DES. In addition, endothelial dysfunction has also been demonstrated adjacent to the BVS, with signs of improvement up to five years after implantation [7–9,14]. Overall, these clinical studies demonstrated impaired adjacent vasomotion in small groups of both DM and non-DM patients, which were too limited to examine the subgroup of DM specifically. However, a relation between DM and early BVS failure has been observed [11]. In addition, none of these studies addressed vascular responsiveness of the untreated vessel as a control. This is relevant since atherosclerosis can also result in endothelial dysfunction, which makes it difficult to directly relate the observed vascular effects to the intervention per se. In the present study, six months of BVS implantation without DM did not affect adjacent endothelial function, which is in accordance with the results found by Gogas et al., one and two years after scaffold implantation in a healthy porcine model [17]. These observations suggest that our findings are specific to BVS combined with DM. Indeed, DM is known to complicate PCI success as shown by a reduced clinical outcome after two years in a large DES-study [26], as well as being an independent predictor of treatment failure up to one year after BVS implantation [11], highlighting again the interaction of DES, including BVS, with DM.

Specifically, in the present study, we showed that the endothelial impairment was caused by a reduced NO-mediated vasodilation. Impairment of NO bioavailability adjacent to DES has been described before [27]. Increased inflammation and oxidative stress due to vascular injury caused by the procedure, drug or other components of the BVS, have been proposed as possible mechanisms [27–29]. While everolimus has been shown to reduce NO-release [30], it is unlikely that the drug is responsible for this effect six months after implantation, as most of it has been released from the scaffold after three months [31]. Other scaffold related processes, including a change in regional wall shear stress and the consequent alterations in local gene expression [32], could also have contributed to the loss of NO synthase activity, although this does not readily explain why this was observed only in the DM + HFD-group. Recently, the AIDA trial was halted after two years due to safety concerns of the BVS with a higher incidence of scaffold thrombosis as compared to the metallic everolimus-coated DES [12]. A recent meta-analysis of all randomized BVS trials to date reported a similar concern for BVS as compared to its DES counterpart in clinical practice [13]. This further indicates

that not the drug everolimus, but the scaffold and its degradation products or the resulting pathology may be responsible for the observed endothelial dysfunction. These effects are thought to extend downstream through accumulation and diffusion within the vasa vasorum, explaining the more pronounced distal effects. Furthermore, DM is known to be strongly associated with NO-mediated endothelial dysfunction [16], although we did not find any evidence of DM-induced altered NO-mediated coronary function within the present model [19,20]. However, combined effects of both BVS and DM might explain the observed reduced NO-availability.

To study the extent of the endothelial dysfunction, we examined small arterial function in the distal perfusion area of the BVS. Previously, we and others have reported distal microvascular dysfunction after first generation DES implantation [3,27]. Therefore, the distal microcirculation is considered at increased risk of dysfunction. Surprisingly, we found an enhanced microvascular endothelium-dependent response, however only in the presence of reduced NO-mediated conduit endothelial function. This effect can be explained by the assumption that the distal microcirculation is reacting to the endothelial dysfunction occurring more proximally. Indeed, the coronary microcirculation is known to enable substantial variations in coronary flow due to several endothelium-dependent regulatory mechanisms including NO, EDHF, and prostacyclins [15]. This heterogeneity supports the concept of compensatory mechanisms that allow substitution of one dilator for another in the presence of disease [33], as shown in the coronary circulation of DM-patients [34]. Therefore, also within the present study, we propose a mechanism of local autoregulation of endothelial function between coronary conduit and small arteries in which a loss of NO-mediated component in the conduit artery is compensated for by NO-, EDHF-, and non-NO/non-EDHF-mediated components in the distal microcirculation.

3.1. Study limitations

Although the present large animal model with cardiovascular risk factors and early atherosclerosis does not completely mimic human obstructive CAD, it allows extensive functional analysis of early alterations in coronary vascular function. However, vascular function was only assessed in vitro. Although it is clear that in vitro several modulators of vascular tone are altered compared to the in vivo situation, including autonomic influences, myocardial metabolism, and blood flow, the in vitro approach allowed us to examine vascular function in parallel and in great detail. In an in vivo setting, such extensive vascular function studies would be hampered both by the potential systemic effects of the various compounds as well as by the long half-life of some of the substances and thus by the interaction of different substances within each animal. Nevertheless, the results from the present study warrant further studies to examine the alterations in endothelial function produced by the BVS in DM in vivo over an extended period of time, in order to assess the longitudinal pattern of coronary vascular impairment following BVS implantation.

A second limitation is that the functional measurements in isolated coronary vessels did not allow pressure fixation of the coronary vascular bed in situ, precluding detailed quantitative investigation of BVS-induced alterations in coronary microvascular structure.

3.2. Conclusions

This is the first study evaluating the effect of six months of BVS-implantation on coronary endothelial function in segments proximal and distal to the BVS. Specifically, in the presence of DM, coronary conduit artery segments located >5 mm distal to the BVS, showed decreased NO-mediated vasodilation. In contrast, the coronary microcirculation in the distal flow area of the BVS showed enhanced endothelium-dependent vasodilation, possibly acting as a compensatory mechanism.

3.3. Perspectives

The present study demonstrates that significant endothelial dysfunction is present in epicardial coronary artery segments located >5 mm proximal or distal to the BVS in diabetic swine on a high fat diet, as late as 6 months after BVS implantation. These observations may explain, at least in part, recent clinical studies reporting late scaffold thrombosis after BVS implantation as well as early treatment failure up to one year after BVS implantation, particularly in diabetic patients.

Conflict of interest

The authors report no relationships that could be construed as a conflict of interest.

Supplementary data to this article can be found online at https://doi.org/10.1016/j.ijcard.2017.11.037.

Acknowledgements

The article is dedicated to Professor W.J. van der Giessen, MD, PhD, who sadly passed away June 6, 2011.

Cindy Niles is kindly acknowledged for performing and analyzing the Oil-red-O staining of the coronary conduit segments.

References

[1] M. Roffi, D.J. Angiolillo, A.P. Kappetein, Current concepts on coronary revascularization in diabetic patients, Eur. Heart J. 32 (22) (2011) 2748–2757.
[2] M. van den Heuvel, O. Sorop, H.M. van Beusekom, W.J. van der Giessen, Endothelial dysfunction after drug-eluting stent implantation, Minerva Cardioangiol. 57 (5) (2009) 629–643.
[3] M. van den Heuvel, O. Sorop, W.W. Batenburg, C.L. Bakker, R. de Vries, S.J. Koopmans, et al., Specific coronary drug-eluting stents interfere with distal microvascular function after single stent implantation in pigs, JACC Cardiovasc. Interv. 3 (7) (2010) 723–730.
[4] E. Gutierrez, A.J. Flammer, L.O. Lerman, J. Elizaga, A. Lerman, F. Fernandez-Aviles, Endothelial dysfunction over the course of coronary artery disease, Eur. Heart J. 34 (41) (2013) 3175–3181.
[5] S. Puricel, Z. Kallinikou, J. Espinola, D. Arroyo, J.J. Goy, J.C. Stauffer, et al., Comparison of endothelium-dependent and -independent vasomotor response after abluminal biodegradable polymer biolimus-eluting stent and persistent polymer everolimus-eluting stent implantation (COMPARE-IT), Int. J. Cardiol. 202 (2016) 525–531.
[6] A. Sumida, B.D. Gogas, H. Nagai, J. Li, S.B. King 3rd, N. Chronos, et al., A comparison of drug eluting stent biocompatibility between third generation NOBORI biolimus A9-eluting stent and second generation XIENCE V everolimus-eluting stent in a porcine coronary artery model, Cardiovasc. Revasc. Med. 16 (6) (2015) 351–357.
[7] P.W. Serruys, Y. Onuma, H.M. Garcia-Garcia, T. Muramatsu, R.J. van Geuns, B. de Bruyne, et al., Dynamics of vessel wall changes following the implantation of the absorb everolimus-eluting bioresorbable vascular scaffold: a multi-imaging modality study at 6, 12, 24 and 36 months, EuroIntervention 9 (11) (2014) 1271–1284.
[8] S. Brugaletta, J.H. Heo, H.M. Garcia-Garcia, V. Farooq, R.J. van Geuns, B. de Bruyne, et al., Endothelial-dependent vasomotion in a coronary segment treated by ABSORB everolimus-eluting bioresorbable vascular scaffold system is related to plaque composition at the time of bioresorption of the polymer: indirect finding of vascular reparative therapy? Eur. Heart J. 33 (11) (2012) 1325–1333.
[9] D. Dudek, L. Rzeszutko, Y. Onuma, Y. Sotomi, R. Depukat, S. Veldhof, et al., Vasomotor response to nitroglycerine over 5 years follow-up after everolimus-eluting bioresorbable scaffold implantation, JACC Cardiovasc. Interv. 10 (8) (2017) 786–795.
[10] P.W. Serruys, J. Ormiston, R.J. van Geuns, B. de Bruyne, D. Dudek, E. Christiansen, et al., A polylactide bioresorbable scaffold eluting everolimus for treatment of coronary stenosis: 5-year follow-up, J. Am. Coll. Cardiol. 67 (7) (2016) 766–776.
[11] D. Capodanno, T. Gori, H. Nef, A. Latib, J. Mehilli, M. Lesiak, et al., Percutaneous coronary intervention with everolimus-eluting bioresorbable vascular scaffolds in routine clinical practice: early and midterm outcomes from the European multicentre GHOST-EU registry, EuroIntervention 10 (10) (2015) 1144–1153.
[12] J.J. Wykrzykowska, R.P. Kraak, S.H. Hofma, R.J. van der Schaaf, E.K. Arkenbout, A.J. IJsselmuiden, et al., Bioresorbable scaffolds versus metallic stents in routine PCI, N. Engl. J. Med. 376 (24) (2017) 2319–2328.
[13] Z.A. Ali, P.W. Serruys, T. Kimura, R. Gao, S.G. Ellis, D.J. Kereiakes, et al., 2-Year outcomes with the Absorb bioresorbable scaffold for treatment of coronary artery disease: a systematic review and meta-analysis of seven randomised trials with an individual patient data substudy, Lancet 390 (10096) (2017) 760–772.
[14] P.W. Serruys, B. Chevalier, Y. Sotomi, A. Cequier, D. Carrie, J.J. Piek, et al., Comparison of an everolimus-eluting bioresorbable scaffold with an everolimus-eluting metallic stent for the treatment of coronary artery stenosis (ABSORB II): a 3 year, randomised, controlled, single-blind, multicentre clinical trial, Lancet 388 (10059) (2016) 2479–2491.

[15] D.J. Duncker, A. Koller, D. Merkus, J.M. Canty Jr., Regulation of coronary blood flow in health and ischemic heart disease, Prog. Cardiovasc. Dis. 57 (5) (2015) 409–422.
[16] C.M. Sena, A.M. Pereira, R. Seica, Endothelial dysfunction - a major mediator of diabetic vascular disease, Biochim. Biophys. Acta 1832 (12) (2013) 2216–2231.
[17] B.D. Gogas, J.J. Benham, S. Hsu, A. Sheehy, D.J. Lefer, T.T. Goodchild, et al., Vasomotor function comparative assessment at 1 and 2 years following implantation of the absorb everolimus-eluting bioresorbable vascular scaffold and the Xience V everolimus-eluting metallic stent in porcine coronary arteries: insights from in vivo angiography, ex vivo assessment, and gene analysis at the stented/scaffolded segments and the proximal and distal edges, JACC Cardiovasc. Interv. 9 (7) (2016) 728–741.
[18] J.P. Lane, L.E. Perkins, A.J. Sheehy, E.J. Pacheco, M.P. Frie, B.J. Lambert, et al., Lumen gain and restoration of pulsatility after implantation of a bioresorbable vascular scaffold in porcine coronary arteries, JACC Cardiovasc. Interv. 7 (6) (2014) 688–695.
[19] O. Sorop, M. van den Heuvel, N.S. van Ditzhuijzen, V.J. de Beer, I. Heinonen, R.W. van Duin, et al., Coronary microvascular dysfunction after long-term diabetes and hypercholesterolemia, Am. J. Physiol. Heart Circ. Physiol. 311 (6) (2016) H1339–H1351.
[20] N.S. van Ditzhuijzen, M. van den Heuvel, O. Sorop, A. Rossi, T. Veldhof, N. Bruining, et al., Serial coronary imaging of early atherosclerosis development in fast-food-fed diabetic and nondiabetic swine, JACC Basic Trans Science 1 (6) (2016) 449–460.
[21] N.S. van Ditzhuijzen, M. Kurata, M. van den Heuvel, O. Sorop, R.W.B. van Duin, I. Krabbendam-Peters, et al., Neoatherosclerosis development following bioresorbable vascular scaffold implantation in diabetic and non-diabetic swine, PLoS One 12 (9) (2017), e0183419.
[22] J.E. van Loon, M.A. Sonneveld, S.F. Praet, M.P. de Maat, F.W. Leebeek, Performance related factors are the main determinants of the von Willebrand factor response to exhaustive physical exercise, PLoS One 9 (3) (2014), e91687.
[23] W.W. Batenburg, R. Popp, I. Fleming, R. de Vries, I.M. Garrelds, P.R. Saxena, et al., Bradykinin-induced relaxation of coronary microarteries: *S*-nitrosothiols as EDHF? Br. J. Pharmacol. 142 (1) (2004) 125–135.
[24] M.C. van Schie, J.E. van Loon, M.P. de Maat, F.W. Leebeek, Genetic determinants of von Willebrand factor levels and activity in relation to the risk of cardiovascular disease: a review, J. Thromb. Haemost. 9 (5) (2011) 899–908.
[25] M. Khairoun, M. van den Heuvel, B.M. van den Berg, O. Sorop, R. de Boer, N.S. van Ditzhuijzen, et al., Early systemic microvascular damage in pigs with atherogenic diabetes mellitus coincides with renal angiopoietin dysbalance, PLoS One 10 (4) (2015), e0121555.
[26] G.W. Stone, E. Kedhi, D.J. Kereiakes, H. Parise, M. Fahy, P.W. Serruys, et al., Differential clinical responses to everolimus-eluting and Paclitaxel-eluting coronary stents in patients with and without diabetes mellitus, Circulation 124 (8) (2011) 893–900.
[27] L.K. Pendyala, J. Li, T. Shinke, S. Geva, X. Yin, J.P. Chen, et al., Endothelium-dependent vasomotor dysfunction in pig coronary arteries with Paclitaxel-eluting stents is associated with inflammation and oxidative stress, JACC Cardiovasc. Interv. 2 (3) (2009) 253–262.
[28] R.P. Juni, H.J. Duckers, P.M. Vanhoutte, R. Virmani, A.L. Moens, Oxidative stress and pathological changes after coronary artery interventions, J. Am. Coll. Cardiol. 61 (14) (2013) 1471–1481.
[29] F. Otsuka, A.V. Finn, S.K. Yazdani, M. Nakano, F.D. Kolodgie, R. Virmani, The importance of the endothelium in atherothrombosis and coronary stenting, Nat. Rev. Cardiol. 9 (8) (2012) 439–453.
[30] S. Banerjee, H. Xu, E. Fuh, K.T. Nguyen, J.A. Garcia, E.S. Brilakis, et al., Endothelial progenitor cell response to antiproliferative drug exposure, Atherosclerosis 225 (1) (2012) 91–98.
[31] J.A. Ormiston, M.W. Webster, G. Armstrong, First-in-human implantation of a fully bioabsorbable drug-eluting stent: the BVS poly-L-lactic acid everolimus-eluting coronary stent, Catheter. Cardiovasc. Interv. 69 (1) (2007) 128–131.
[32] C.V. Bourantas, H.M. Garcia-Garcia, C.A. Campos, Y.J. Zhang, T. Muramatsu, M.A. Morel, et al., Implications of a bioresorbable vascular scaffold implantation on vessel wall strain of the treated and the adjacent segments, Int. J. Card. Imaging 30 (3) (2014) 477–484.
[33] A.M. Beyer, D.D. Gutterman, Regulation of the human coronary microcirculation, J. Mol. Cell. Cardiol. 52 (4) (2012) 814–821.
[34] Z. Bagi, A. Feher, T. Beleznai, Preserved coronary arteriolar dilatation in patients with type 2 diabetes mellitus: implications for reactive oxygen species, Pharmacol. Rep. 61 (1) (2009) 99–104.

Please cite this article as: M. van den Heuvel, et al., The effect of bioresorbable vascular scaffold implantation on distal coronary endothelial function in dyslipidemic swine with and ..., Int J Cardiol (2017), https://doi.org/10.1016/j.ijcard.2017.11.037